A symbolic approach for the efficient computation of transfer functions in two-ports*

Ricardo Riaza†

Abstract

We present in this paper a number of formulae to compute all four transfer functions of a two-port in a uniform and efficient manner. Our approach improves on previous results by substantially reducing the order of the matrices involved in the computations. We handle circuit elements which may not have an admittance description: not only devices described in impedance terms, but also for instance the ones arising in the small-signal equivalents of operational amplifiers. In greater generality, we may accommodate devices without specifying *a priori* any control variables for their characteristics. Our framework avoids the need to use ad-hoc techniques depending on the form of the devices' characteristics, with all four transfer functions addressed in the same manner. Classical and generalized cofactors formulae are derived as particular cases. We apply the results to the analysis of active filters: in this context, both ideal and nonideal op-amps can be treated in a uniform manner, and the computation of certain sensitivities turns out to be possible because of the availability of explicit analytical expressions for the transfer functions.

Keywords: linear circuit, two-port, homogeneous coordinates, transfer function, cofactors formulae, operational amplifier, active filter, VCVS filter, Sallen-Key filter, KHN filter.

1 Introduction

In essence, the use of cofactors formulae in linear circuit theory is already present in the pioneering work of Kirchhoff and Maxwell in the 19th century [16, 19]. In order to present the main ideas in a simple context, let us consider a connected linear circuit with n nodes and m branches excited by a single independent current source operating in sinusoidal steady state. Choose the reference node as one of the terminals of the current source and, for later use, assume that the other terminal node is the α-th one (cf. Figure 1).

Assume additionally that the voltage-current characteristics of the remaining circuit devices do not depend on the voltage or the current at the branch accommodating the source and that they can be described in terms of an $(m-1)\times(m-1)$ branch-admittance matrix Y. This matrix would be diagonal for (let us say) uncoupled circuits, but not in the presence

*This is the author's original, pre-peer-reviewed version of the manuscript.

†The author is with the Depto. de Matemática Aplicada a las TIC, ETS Ingenieros de Telecomunicación, and the Information Processing and Telecommunications Center, Universidad Politécnica de Madrid, Spain. *ricardo.riaza@upm.es*, https://orcid.org/0000-0003-0868-4446.

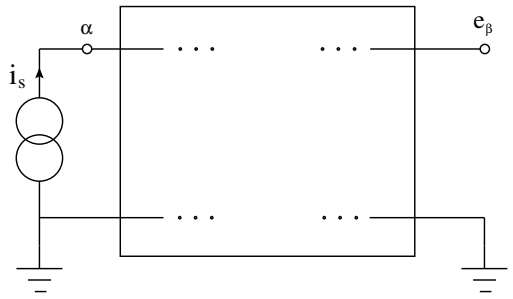


Figure 1: Generic circuit to illustrate the use of cofactors formulae.

of controlled sources and/or coupling effects. Let A be the reduced incidence matrix of the digraph obtained after the removal of the source, and e stand for the $(n-1)$-dimensional vector defined by the potentials at all nodes but the reference one. With this setup, the circuit equations read as

$$AYA^{\mathsf{T}}e = f, \tag{1}$$

where f is an $(n-1)$-dimensional vector whose only nonzero entry equals the phasor of the current injected by the source, to be written as i_s, at the α-th position. The coefficient matrix of (1) is the well-known node-admittance matrix. The potential at node β is then found by Cramer's rule to be

$$e_\beta = \frac{\Delta_{\alpha\beta}}{\Delta} i_s, \tag{2}$$

where Δ is the determinant of the node-admittance matrix and $\Delta_{\alpha\beta}$ is the cofactor of its (α, β)-entry. This is of course well-known in classical circuit theory and the above setting can be found e.g. in [28].

The scope of the approach above, which basically amounts to computing a transfer impedance, can be enlarged to a certain extent. Specifically, the assumption that the source is incident with the reference node can be removed and, similarly, the output voltage can be defined by an arbitrary pair of nodes. Some natural amendments are needed to handle these situations: we refer the reader e.g. to [21, Chapter 8] for a detailed analysis, again under the assumption that the circuit can be described in terms of the node-admittance matrix. Dealing with nonideal sources also involves some technicalities. But the computation of other transfer functions turns out to be more intricate, and the accommodation of devices which are not voltage-controlled becomes increasingly complex. These difficulties also show up when using the indefinite admittance matrix: we refer the reader to [5, Chapter 2] as a sample of the heuristics needed to deal e.g. with nonideal operational amplifiers from this standpoint. In general, the use of the indefinite impedance matrix [5, Chapter 11] but also the approach based on generalized cofactors [4, 5] still lack generality since, in all cases, either an impedance or an admittance description is assumed to hold for all devices simultaneously.

Broadly speaking, these difficulties can be seen as a consequence of the wish to use reduced descriptions *too early* in the modeling process. In rough terms, the reduced size of nodal analysis models is very convenient in circuit simulation, but requires a number of amendments here and there in order to deal with devices which are not voltage-controlled, and also to handle all four types of transfer functions. Somehow, the use of reduced models always

comes with certain "associated" working assumptions which may not be met in practice, and handling the corresponding exceptions complicates the analysis. In this regard, we have mentioned nodal analysis above, but the same drawback is met when using current-controlled descriptions to set up the indefinite impedance matrix, and the same happens when defining the generalized cofactors in terms of the cutset-admittance or the loop-impedance matrices. Detailed discussions can be found in the aforementioned books [4, 5].

We propose in this paper a different strategy for the symbolic computation of transfer functions in a general but at the same time efficient manner. Along the lines proposed in [22, 23], we use homogeneous models to obtain symbolic expressions for all four types of transfer functions in a truly general manner, that is, without any *a priori* assumptions on the form of the characteristics of all circuit devices. In its seminal form, these models use a reduced incidence matrix or a reduced cutset matrix together with a reduced cycle matrix for the description of Kirchhoff laws. Background on the fundamentals of such models is presented in Section 2. Only in a second step we provide expressions for the numerator and the denominator of the transfer functions in terms of reduced-order circuit matrices, involving only incidence or cutset matrices in the description of the circuit topology. This way we get rid of the use of cycle matrices in the models without losing generality, thereby improving on the results presented in [23]. Details are provided in Section 3, which contains the main results of the paper. We will obtain explicit formulae for all types of transfer functions, accommodating in particular ideal and nonideal sources as well as arbitrary loads in a comprehensive manner. The aforementioned generalized cofactors formulae of [4, 5], as well as classical formulae holding in simpler settings such as the one at the beginning of this section, will be shown to hold as particular cases. We then apply our framework to actual circuit analysis by focusing on active filters in Section 4. For illustration, using nonideal models of the operational amplifier, we examine how the peak frequency of different filters depends on the parameters of the op-amps. Some concluding remarks can be found in Section 5. In the Appendix we briefly compile some auxiliary concepts and results from digraph theory.

2 Background

2.1 Homogeneous description of linear devices

The homogeneous approach proposed in [22] stems from the description of Ohm's law for a single immittance in the implicit form

$$pv - qi = 0, \tag{3}$$

where the complex parameters p and q do not vanish simultaneously. Provided that $p \neq 0$, one may resort to the classical impedance (or current-controlled) form $v = zi$, with $z = q/p$. If $q \neq 0$, then (3) can be rewritten in the voltage-controlled form $i = yv$, where $y = p/q$ is the admittance.

The idea of using (3), without resorting to these classical forms, is to retain generality in the modeling process, since both the impedance and the admittance descriptions necessarily lack generality. Just note that an open-circuit (resp. a short-circuit) does not admit an impedance (resp. admittance) description. Needless to say, this is aimed at a symbolic analysis since for concrete numerical values one may always resort to a classical description. Notice that, in

(3), p and q are defined only up to a nonvanishing multiplicative constant: for this reason, these parameters define the homogeneous coordinates of a point in a complex projective line. In rough terms, only the ratio between p and q matters. Accordingly, we borrow the notation $(p : q)$ from projective geometry to describe the device. General background on projective geometry can be found in [8, 10, 24].

In order to accommodate independent sources, we may extend the expression depicted in (3) by writing

$$pv - qi = s, \tag{4}$$

with $(p, q) \neq (0, 0)$, as before, and $s \neq 0$. Now, the assumption $p \neq 0$ supports describing the source as a voltage source, since (4) can be recast as

$$v - zi = v_s, \tag{5}$$

with $z = q/p$ and $v_s = s/p$. In particular, an ideal voltage source is defined by the conditions $p \neq 0 \neq s$, $q = 0$, the latter yielding $z = 0$. Analogously, if $q \neq 0$ then the abstract source defined by (4) can be described as a current source via

$$yv - i = i_s, \tag{6}$$

with $y = p/q$, $i_s = s/q$ in this case. An ideal current source is defined by the assumptions $p = 0$, $q \neq 0 \neq s$. For later use, let us emphasize that the relations $pv_s = s$ and $qi_s = s$ hold for sources admitting a description as a voltage source ($p \neq 0$) or as a current source ($q \neq 0$), respectively, and that this applies to both ideal and nonideal sources.

Coupled devices and controlled sources. The same idea can be used to describe a set of linear devices, possibly displaying coupling effects and/or including dependent sources. In general, for m devices one may write

$$Pv - Qi = s \tag{7}$$

to describe the whole set of characteristics. Here P and Q are $m \times m$ matrices and s is an m-dimensional vector of excitations. Needless to say, uncoupled devices or independent sources lead to diagonal blocks within the matrices P and Q. In most cases, coupled devices and dependent sources involve just two linear elements and this yields 2×2 blocks in the matrices P and Q. In particular, this is the case for operational amplifiers, as discussed below.

Operational amplifiers. We will use the framework above for the analysis of active filters in Section 4. To this aim, let us detail here the form that the small-signal model of an operational amplifier takes (find e.g. in [9, 11, 14, 15] general background on the theory of operational amplifiers). We refer the reader to Figure 2.

Elementary circuit analysis yields the relations $i_1 = G_i v_1$, $v_2 = av_1 + R_0 i_2$, where a is the open-loop gain of the amplifier and G_i and R_0 are the input conductance and the output resistance, respectively. We use a conductance description for the input immittance in order to accommodate the ideal case simply as $G_i = 0$. To account for the infinite gain case, let use recast the second relation above as $v_1 = b(v_2 - R_0 i_2)$, with $b = 1/a$. The infinite gain case corresponds to $b = 0$. We may therefore describe the device, both in the ideal and the nonideal cases, by means of the relation $Pv - Qi = 0$, with

$$P = \begin{pmatrix} G_i & 0 \\ -1 & b \end{pmatrix}, \; Q = \begin{pmatrix} 1 & 0 \\ 0 & bR_0 \end{pmatrix} \tag{8}$$

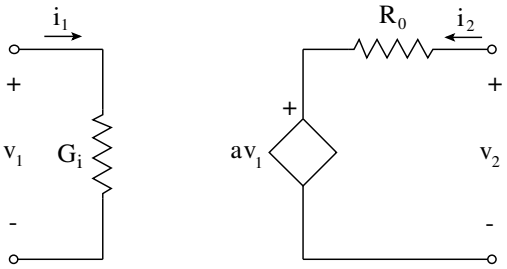


Figure 2: Op-amp equivalent model.

or, by splitting $i = (i_1, i_2)$, $v = (v_1, v_2)$, as

$$\begin{pmatrix} -1 & 0 & G_i & 0 \\ 0 & -bR_0 & -1 & b \end{pmatrix} \begin{pmatrix} i_1 \\ i_2 \\ v_1 \\ v_2 \end{pmatrix} = 0.$$

The infinite gain case, defining an ideal op-amp, yields a nullator-norator pair, since the equations above are easily seen to amount to $i_1 = 0$, $v_1 = 0$. The values of G_i and R_0 are immaterial in this case. We emphasize the fact that the ideal op-amp does not need a separate treatment; one just needs to annihilate the b-parameter to accommodate the ideal case.

2.2 Homogeneous circuit models

By letting (7) describe the characteristics of the whole set of devices, the equations of a linear, connected circuit with n nodes and m branches turn out to read as

$$\begin{pmatrix} A & 0 \\ 0 & B \\ -Q & P \end{pmatrix} \begin{pmatrix} i \\ v \end{pmatrix} = \begin{pmatrix} 0 \\ 0 \\ s \end{pmatrix}. \tag{9}$$

Here A and B are $(n-1)\times m$ and $(m-n+1)\times m$ matrices with entries in $\{0, +1, -1\}$ describing Kirchhoff's laws in the form $Ai = 0$ and $Bv = 0$, where i and v are the m-dimensional vectors of branch currents and branch voltages. Typically, A is a reduced incidence matrix (or a reduced cutset matrix) and B is a reduced cycle matrix of the digraph obtained after endowing all circuit branches with an orientation. We refer the reader to [2, 3, 4, 6] for the necessary background on graph theory and, specifically, for detailed discussions of the main properties of these matrices. Some specific properties of these matrices, to be used in later analyses, are compiled in the Appendix.

Two-ports. Throughout the paper we will apply the formalism above to the analysis of two-ports. Specifically, we will consider connected linear circuits with two distinguished branches (or *ports*), namely an input and an output. We may assume that the input and the output correspond to branches 1 and 2, respectively, without loss of generality. As above, A will stand for any reduced incidence matrix or any reduced cutset matrix of the digraph underlying the circuit. Moreover, we will let A_1, A_2 and A_r stand for the submatrices defined respectively

by the first, the second and the remaining $m-2$ columns of A. We will accordingly split the current vector as $i = (i_1,\, i_2,\, i_r)$; note that i_r comprises $m-2$ components. Similarly, B will be any reduced cycle matrix, and we will split both B and v exactly as above to write $B = \begin{pmatrix} B_1 & B_2 & B_r \end{pmatrix}$ and $v = (v_1,\, v_2,\, v_r)$.

We will assume that the internal circuit branches do not accommodate independent sources and do not display any coupling effects with the ports; this means that the internal branches are described by a set of characteristics that can be written in the form $P_r v_r - Q_r i_r = 0$ for certain $(m-2)\times(m-2)$ matrices P_r, Q_r. Together with the characteristics of the devices connected at the ports, this will define the P and Q blocks within the model (9), as detailed in the following section.

3 Symbolic computation of transfer functions

The background material presented above paves the way for the discussion of the core results of the paper, to be presented in this section. The two main results are Theorem 1 and Theorem 2. Theorem 1 provides explicit expressions for the transfer functions involving only a reduced cutset (or incidence) matrix, getting rid of the cycle matrix without losing generality. This result does not put any restriction on the controlling variables of the different devices and provides the transfer functions in terms of their p- and q-parameters; the example in Section 3.2 should be of help in this direction. In turn, Theorem 2 shows how to further reduce the size of the matrices involved in the computations when some (not necessarily all) of the internal devices are given an admittance description, as it is the case in most practical circuits.

3.1 Transfer functions using homogeneous descriptions of two-ports

Let the input port (assumed for the moment to correspond to branch 1) accommodate an independent source, described by a relation of the form $p_1 v_1 - q_1 i_1 = s_1$ with $(p_1, q_1) \neq (0,0)$. Later on we will particularize the results to cases in which the source is given a classical description, either as a voltage source (provided that $p_1 \neq 0$) or as a current source (when $q_1 \neq 0$). Additionally, the output (branch 2) accommodates an uncoupled load described in homogeneous form by the relation $p_2 v_2 - q_2 i_2 = 0$, again with $(p_2, q_2) \neq (0,0)$.

With this setup, the model (9) takes the form

$$\begin{pmatrix} A_1 & A_2 & A_r & 0 & 0 & 0 \\ 0 & 0 & 0 & B_1 & B_2 & B_r \\ -q_1 & 0 & 0 & p_1 & 0 & 0 \\ 0 & -q_2 & 0 & 0 & p_2 & 0 \\ 0 & 0 & -Q_r & 0 & 0 & P_r \end{pmatrix} \begin{pmatrix} i_1 \\ i_2 \\ i_r \\ v_1 \\ v_2 \\ v_r \end{pmatrix} = \begin{pmatrix} 0 \\ 0 \\ s_1 \\ 0 \\ 0 \end{pmatrix}. \tag{10}$$

Now, the different transfer functions can be obtained by expressing the circuit output (either v_2 or i_2) in terms of the excitation s_1. The point is that our formulation makes it possible to do this in broad generality, for two reasons: first, no restriction has been placed on the characteristics of the circuit devices (in particular, no assumption has been made on the existence of a voltage-controlled description, as it is often made when using nodal analysis); second, all four transfer functions will be expressed symbolically in a unique statement. This is the content of Theorem 1. This result states that, regardless of the form of the devices'

characteristics, the computation of all transfer functions essentially amounts to computing the two determinants arising in (11). Notice that an efficient computation turns out to be possible by expressing these determinants just in terms of a reduced incidence matrix (or a reduced cutset matrix, even if for the sake of simplicity the incidence matrix is a more natural choice). Several consequences of this result will be discussed later on.

Some remarks are in order before stating the result. Let us mention that, when the input and the ouput correspond to arbitrary branches (say j and k, respectively), the amendments in the system (10) are rather obvious; we just assumed $j = 1$ and $k = 2$ there to avoid a cumbersome splitting of the A, B, P and Q blocks within the coefficient matrix. It is worth emphasizing, however, that the analysis that follows applies to the general case (that is, with arbitrary j and k, as long as $j \neq k$) and, for the sake of completeness, we state the results in this general setup. In this context, the vectors i_r and v_r comprise all currents and voltages exception made of those at the ports; similarly, A_r and B_r are defined by all columns of A and B but the j-th and k-th ones. Also, let us recall that the assumptions $p_j \neq 0$ and $q_j \neq 0$ are necessary for the independent source to admit a description as a voltage source or as a current source, with the relations $v_{s_j} = s_j/p_j$ and $i_{s_j} = s_j/q_j$ holding in either case (cf. Section 2.1). For this reason, either one of these two conditions (namely, $p_j \neq 0$ or $q_j \neq 0$) is necessary for the corresponding transfer functions in (12) to be well-defined.

Theorem 1. *Consider a connected linear circuit with two distinguished branches, namely an input branch j, which is the only one accommodating an independent source, governed by*

$$p_j v_j - q_j i_j = s_j,$$

and an output branch k, with an uncoupled load defined by the characteristic

$$p_k v_k - q_k i_k = 0.$$

The conditions $(p_j, q_j) \neq (0, 0)$, $s_j \neq 0$ and $(p_k, q_k) \neq (0, 0)$ are assumed to hold. We also assume that the characteristics of the remaining circuit branches do not depend on the input/output voltage and current, and therefore can be written as

$$P_r v_r - Q_r i_r = 0,$$

for certain square matrices P_r, Q_r of order $m - 2$. For an arbitrary choice of the reduced incidence matrix (or reduced cutset matrix) A, write

$$\eta = \det \begin{pmatrix} 0 & A_j & A_r \\ -A_k^{\mathsf{T}} & 0 & 0 \\ -P_r A_r^{\mathsf{T}} & 0 & Q_r \end{pmatrix}, \quad \zeta = \det \begin{pmatrix} 0 & A_j & A_k & A_r \\ -p_j A_j^{\mathsf{T}} & q_j & 0 & 0 \\ -p_k A_k^{\mathsf{T}} & 0 & q_k & 0 \\ -P_r A_r^{\mathsf{T}} & 0 & 0 & Q_r \end{pmatrix}. \tag{11}$$

Assuming that ζ is not identically zero as a function of the parameters p_j, q_j, p_k, q_k, the four transfer functions from branch j to branch k can be expressed as

$$\frac{v_k}{v_{s_j}} = p_j q_k \frac{\eta}{\zeta}, \qquad \frac{i_k}{v_{s_j}} = p_j p_k \frac{\eta}{\zeta}, \qquad \frac{v_k}{i_{s_j}} = q_j q_k \frac{\eta}{\zeta}, \qquad \frac{i_k}{i_{s_j}} = q_j p_k \frac{\eta}{\zeta}, \tag{12}$$

provided that $p_j \neq 0$ in the first two cases and $q_j \neq 0$ in the last two.

The proof of Theorem 1 will be based on the following auxiliary result, which in essence shows how to get rid of the reduced cycle matrix B in the computation of the functions η and ζ. Compare the size of the matrices within eq. (13) below: the orders are $2m$ and $m+n-1$ for the matrices on the left-hand side and the right-hand side, respectively (and be aware that $n \ll m$ in most practical circuits). This result makes use of certain integer constants related to the matrices describing the digraph and whose definition and meaning are discussed in the Appendix.

Lemma 1. *For arbitrary $m \times m$ matrices P, Q,*

$$\det \begin{pmatrix} A & 0 \\ 0 & B \\ -Q & P \end{pmatrix} = \frac{k_{\mathrm{AB}}}{k_{\mathrm{A}}^2} \det \begin{pmatrix} 0 & A \\ -PA^{\mathsf{T}} & Q \end{pmatrix}, \tag{13}$$

where k_{AB} and k_{A} are defined in (49)-(50).

Proof. Here we use the well-known property $BA^{\mathsf{T}} = 0$, which expresses the orthogonality between the cut space and the cycle space (cf. [2, 3, 4]), to write

$$\begin{pmatrix} A & 0 \\ 0 & B \\ -Q & P \end{pmatrix} \begin{pmatrix} I_m & 0 & * \\ 0 & A^{\mathsf{T}} & B^{\mathsf{T}}(BB^{\mathsf{T}})^{-1} \end{pmatrix} = \begin{pmatrix} A & 0 & * \\ 0 & 0 & I_{m-n+1} \\ -Q & PA^{\mathsf{T}} & * \end{pmatrix}. \tag{14}$$

The $*$ symbols denote blocks whose actual content is immaterial. Now, $m(m-n+1) = m(m+1) - mn$ (a number with the same parity as mn) row swaps show that the determinant of the last matrix equals

$$(-1)^{mn} \det \begin{pmatrix} A & 0 \\ -Q & PA^{\mathsf{T}} \end{pmatrix}.$$

Within this matrix, m sign changes in the last rows and $m(n-1)$ column swaps show (using $m + m(n-1) = mn$) that

$$\det \begin{pmatrix} A & 0 & * \\ 0 & 0 & I_{m-n+1} \\ -Q & PA^{\mathsf{T}} & * \end{pmatrix} = \det \begin{pmatrix} 0 & A \\ -PA^{\mathsf{T}} & Q \end{pmatrix}. \tag{15}$$

Therefore, in order to prove (13) it just remains to show that the second factor in the left-hand side of (14) accounts for the constants arising in (13). Specifically, we need to prove that

$$\det \begin{pmatrix} I_m & 0 & * \\ 0 & A^{\mathsf{T}} & B^{\mathsf{T}}(BB^{\mathsf{T}})^{-1} \end{pmatrix} = \det \begin{pmatrix} A^{\mathsf{T}} & B^{\mathsf{T}}(BB^{\mathsf{T}})^{-1} \end{pmatrix} \tag{16}$$

equals $k_{\mathrm{A}}^2/k_{\mathrm{AB}}$. To do so, write the transpose of the last matrix in (16) as

$$\begin{pmatrix} A \\ (BB^{\mathsf{T}})^{-\mathsf{T}} B \end{pmatrix} = \begin{pmatrix} I_{n-1} & 0 \\ 0 & (BB^{\mathsf{T}})^{-\mathsf{T}} \end{pmatrix} \begin{pmatrix} A \\ B \end{pmatrix},$$

which yields

$$\det \begin{pmatrix} A^{\mathsf{T}} & B^{\mathsf{T}}(BB^{\mathsf{T}})^{-1} \end{pmatrix} = (\det \left(BB^{\mathsf{T}}\right))^{-1} \det \begin{pmatrix} A \\ B \end{pmatrix} = \frac{k_{\mathrm{AB}}}{k_{\mathrm{B}}^2}, \tag{17}$$

using (52) and (53) in the last step. The identity (13) then follows from (14), (15) and (17) together with the fact that $k_{\mathrm{AB}}/k_{\mathrm{B}}^2 = k_{\mathrm{A}}^2/k_{\mathrm{AB}}$, as detailed in the Appendix. □

Proof of Theorem 1. Without loss of generality we may assume $j = 1$, $k = 2$, what avoids several cumbersome details when splitting the different matrices arising in the proof. We emphasize, however, that our claims apply to two-ports with an arbitrary input j and an arbitrary output $k \neq j$.

Assume first that we want to express the output voltage, v_2, in terms of the excitation at the input, be it supplied by a current or a voltage source (either ideal or nonideal, in both cases). This requires solving for v_2 in (10). Cramer's rule yields a quotient whose numerator is the determinant

$$\det\begin{pmatrix} A_1 & A_2 & A_r & 0 & 0 & 0 \\ 0 & 0 & 0 & B_1 & 0 & B_r \\ -q_1 & 0 & 0 & p_1 & s_1 & 0 \\ 0 & -q_2 & 0 & 0 & 0 & 0 \\ 0 & 0 & -Q_r & 0 & 0 & P_r \end{pmatrix} = q_2 s_1 \det\begin{pmatrix} A_1 & A_2 & A_r & 0 & 0 & 0 \\ 0 & 0 & 0 & B_1 & B_2 & B_r \\ 0 & 0 & 0 & 0 & 1 & 0 \\ 0 & -1 & 0 & 0 & 0 & 0 \\ 0 & 0 & -Q_r & 0 & 0 & P_r \end{pmatrix}, \tag{18}$$

where we have used elementary properties of determinants from linear algebra. It is worth noting that the matrix in the right-hand side is the coefficient matrix of the two-port terminated by a norator at the input and a nullator at the output. The two key determinants in our analysis are, therefore,

$$\eta_{\mathrm{AB}} = \det\begin{pmatrix} A_1 & A_2 & A_r & 0 & 0 & 0 \\ 0 & 0 & 0 & B_1 & B_2 & B_r \\ 0 & 0 & 0 & 0 & 1 & 0 \\ 0 & -1 & 0 & 0 & 0 & 0 \\ 0 & 0 & -Q_r & 0 & 0 & P_r \end{pmatrix},\ \zeta_{\mathrm{AB}} = \det\begin{pmatrix} A_1 & A_2 & A_r & 0 & 0 & 0 \\ 0 & 0 & 0 & B_1 & B_2 & B_r \\ -q_1 & 0 & 0 & p_1 & 0 & 0 \\ 0 & -q_2 & 0 & 0 & p_2 & 0 \\ 0 & 0 & -Q_r & 0 & 0 & P_r \end{pmatrix}, \tag{19}$$

the latter providing the denominator in Cramer's rule. On account of the identities $s_1 = p_1 v_{s_1}$ for voltage sources (for which $p_1 \neq 0$) and $s_1 = q_1 i_{s_1}$ for current sources (with $q_1 \neq 0$ holding in this case), we may then write

$$\frac{v_2}{v_{s_1}} = p_1 q_2 \frac{\eta_{\mathrm{AB}}}{\zeta_{\mathrm{AB}}}, \quad \frac{v_2}{i_{s_1}} = q_1 q_2 \frac{\eta_{\mathrm{AB}}}{\zeta_{\mathrm{AB}}}. \tag{20}$$

Proceeding in the same manner we get

$$\frac{i_2}{i_{s_1}} = q_1 p_2 \frac{\eta_{\mathrm{AB}}}{\zeta_{\mathrm{AB}}}, \quad \frac{i_2}{v_{s_1}} = p_1 p_2 \frac{\eta_{\mathrm{AB}}}{\zeta_{\mathrm{AB}}}. \tag{21}$$

It remains to show that the ratio $\eta_{\mathrm{AB}}/\zeta_{\mathrm{AB}}$ amounts to η/ζ, with η and ζ given in (11) (after setting $j = 1$, $k = 2$ there). We use Lemma 1 for this: note, indeed, that the two matrices in (19) have the form arising in the left-hand side of (13). For the matrix defining η_{AB} in (19), let

$$P = \begin{pmatrix} 0 & 1 & 0 \\ 0 & 0 & 0 \\ 0 & 0 & P_r \end{pmatrix}, \quad Q = \begin{pmatrix} 0 & 0 & 0 \\ 0 & 1 & 0 \\ 0 & 0 & Q_r \end{pmatrix} \tag{22}$$

and, after elementary computations, the matrix in the right-hand side of (13) reads as

$$\begin{pmatrix} 0 & A_1 & A_2 & A_r \\ -A_2^{\mathsf{T}} & 0 & 0 & 0 \\ 0 & 0 & 1 & 0 \\ -P_r A_r^{\mathsf{T}} & 0 & 0 & Q_r \end{pmatrix}. \tag{23}$$

The determinant of this matrix is easily seen to amount to

$$\begin{pmatrix} 0 & A_1 & A_r \\ -A_2^{\mathsf{T}} & 0 & 0 \\ -P_r A_r^{\mathsf{T}} & 0 & Q_r \end{pmatrix}. \tag{24}$$

With arbitrary input and output j and k, this provides the expression given for η in (11).

The analysis for ζ_{AB} is entirely analogous. In this case we have

$$P = \begin{pmatrix} p_1 & 0 & 0 \\ 0 & p_2 & 0 \\ 0 & 0 & P_r \end{pmatrix}, \quad Q = \begin{pmatrix} q_1 & 0 & 0 \\ 0 & q_2 & 0 \\ 0 & 0 & Q_r \end{pmatrix} \tag{25}$$

and the matrix arising in the right-hand side of (13) is now

$$\begin{pmatrix} 0 & A_1 & A_2 & A_r \\ -p_1 A_1^{\mathsf{T}} & q_1 & 0 & 0 \\ -p_2 A_2^{\mathsf{T}} & 0 & q_2 & 0 \\ -P_r A_r^{\mathsf{T}} & 0 & 0 & Q_r \end{pmatrix}. \tag{26}$$

Again, for arbitrary j, k we get the expression defining ζ in (11). Altogether, this shows that the quotient $\eta_{\text{AB}}/\zeta_{\text{AB}}$ amounts to η/ζ, since the coefficient $k_{\text{AB}}/k_{\text{A}}^2$ in the right-hand side of (13) is the same for the two matrices displayed in (19). □

3.2 Example

We will use the circuit depicted in Figure 3 for illustration, mainly to help the reader follow the main ideas introduced above. For simplicity we do not include any coupling effects in the example. The goal is to show how our framework allows for a truly general description of transfer functions, and also to illustrate how to apply the results to circuits with classical descriptions, simply by tuning certain parameters to the appropriate values. More elaborate examples, coming from actual circuit analysis, will be discussed in Section 4.

The circuit in Figure 3 is inspired in the example discussed in [4, Ex. 2.9, pp. 105-106], where the goal is to compute either the transfer admittance or the transfer impedance from the input (A in the figure) to the output (B). In the aforementioned book, two different analyses are necessary to carry out both computations, using loop analysis to obtain the transfer admittance and cutset analysis for the transfer impedance. We propose instead a unique, comprehensive analysis to cover actually all four transfer functions.

The input branch, labeled as A, accommodates a possibly nonideal abstract source (later on we will give it classical descriptions involving two branches, to be numbered as 1 and 2: hence the A label in the figure). Write its characteristic as

$$p_a v_a - q_a i_a = s_a,$$

with $(p_a, q_a) \neq (0,0)$, $s_a \neq 0$. The output branch, B, as well as branches 3 and 4 are immittances, to be described by the homogeneous parameters $(p_b : q_b)$, $(p_3 : q_3)$ and $(p_4 : q_4)$, respectively; again, we assume that all (p_b, q_b), (p_3, q_3) and (p_4, q_4) are different from $(0,0)$.

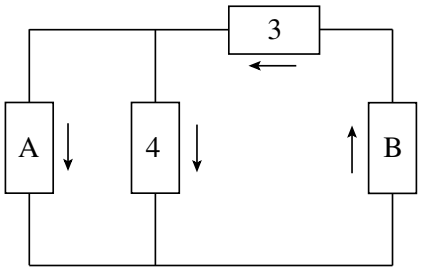


Figure 3: Example.

In the topological description of the circuit we will use the reduced incidence matrix A defined by the reference directions in Figure 3, with the top left and top right nodes being nodes 1 and 2, while the one at the bottom is the reference node. Hence

$$A = \begin{pmatrix} 1 & 0 & -1 & 1 \\ 0 & -1 & 1 & 0 \end{pmatrix}. \tag{27}$$

Below, we denote by A_a, A_b, A_3 and A_4 the first, second, third and fourth columns of this matrix, respectively.

All four transfer functions can be obtained in a straightforward manner in terms of the determinants η and ζ depicted in (11), which in this case read as

$$\eta = \det \begin{pmatrix} 0 & A_a & A_3 & A_4 \\ -A_b^{\mathsf{T}} & 0 & 0 & 0 \\ -p_3 A_3^{\mathsf{T}} & 0 & q_3 & 0 \\ -p_4 A_4^{\mathsf{T}} & 0 & 0 & q_4 \end{pmatrix} = \det \begin{pmatrix} 0 & 0 & 1 & -1 & 1 \\ 0 & 0 & 0 & 1 & 0 \\ 0 & 1 & 0 & 0 & 0 \\ p_3 & -p_3 & 0 & q_3 & 0 \\ -p_4 & 0 & 0 & 0 & q_4 \end{pmatrix}$$

and

$$\zeta = \det \begin{pmatrix} 0 & A_a & A_b & A_3 & A_4 \\ -p_a A_a^{\mathsf{T}} & q_a & 0 & 0 & 0 \\ -p_b A_b^{\mathsf{T}} & 0 & q_b & 0 & 0 \\ -p_3 A_3^{\mathsf{T}} & 0 & 0 & q_3 & 0 \\ -p_4 A_4^{\mathsf{T}} & 0 & 0 & 0 & q_4 \end{pmatrix} = \det \begin{pmatrix} 0 & 0 & 1 & 0 & -1 & 1 \\ 0 & 0 & 0 & -1 & 1 & 0 \\ -p_a & 0 & q_a & 0 & 0 & 0 \\ 0 & p_b & 0 & q_b & 0 & 0 \\ p_3 & -p_3 & 0 & 0 & q_3 & 0 \\ -p_4 & 0 & 0 & 0 & 0 & q_4 \end{pmatrix},$$

taking the expressions

$$\eta = -p_3 q_4, \quad \zeta = p_a p_3 q_4 q_b + p_a q_3 q_4 p_b + q_a p_3 p_4 q_b + q_a p_3 q_4 p_b + q_a q_3 p_4 p_b.$$

Note that ζ provides the network determinant for the circuit in Figure 3 with arbitrary terminations at the ports. As detailed in [22] (with the results, in essence, tracing back to

the seminal work of Kirchhoff himself, cf. [16]), in this uncoupled setting this determinant is known to enumerate the circuit spanning trees, with the p- and the q- factors signaling the tree/cotree branches within each term. We suggest the reader to check the details.

From the formulae depicted in (12) and the expressions obtained above, the four transfer functions are

$$\frac{v_b}{v_{s_a}} = \frac{-p_a q_b p_3 q_4}{p_a p_3 q_4 q_b + p_a q_3 q_4 p_b + q_a p_3 p_4 q_b + q_a p_3 q_4 p_b + q_a q_3 p_4 p_b} \tag{28}$$

$$\frac{i_b}{v_{s_a}} = \frac{-p_a p_b p_3 q_4}{p_a p_3 q_4 q_b + p_a q_3 q_4 p_b + q_a p_3 p_4 q_b + q_a p_3 q_4 p_b + q_a q_3 p_4 p_b} \tag{29}$$

$$\frac{v_b}{i_{s_a}} = \frac{-q_a q_b p_3 q_4}{p_a p_3 q_4 q_b + p_a q_3 q_4 p_b + q_a p_3 p_4 q_b + q_a p_3 q_4 p_b + q_a q_3 p_4 p_b} \tag{30}$$

$$\frac{i_b}{i_{s_a}} = \frac{-q_a p_b p_3 q_4}{p_a p_3 q_4 q_b + p_a q_3 q_4 p_b + q_a p_3 p_4 q_b + q_a p_3 q_4 p_b + q_a q_3 p_4 p_b}. \tag{31}$$

Worth emphasizing is that this holds regardless of the ideal or nonideal nature of sources, on the one hand, and applies to arbitrary loads, on the other. All possible assumptions on internal immittances are also captured, including the cases in which they amount to a short- or open-circuit. The cases in which the different devices are given classical descriptions are captured simply by tuning conveniently certain parameters in the expressions just obtained.

For illustration, let us consider the case in which all devices are given a current-controlled description; this means that the source can be described as a (possibly nonideal) voltage source, and that all three immittances can be given an impedance description. Cf. Figure 4 (which corresponds to Fig. 2.25 in [4, p. 104]).

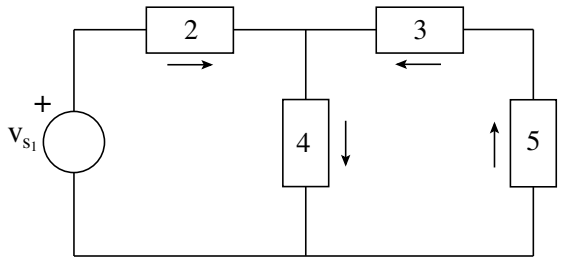


Figure 4: Describing the source as a voltage source.

This setup is obtained by choosing $p_a = p_3 = p_4 = p_b = 1$, $q_a = z_2$, $q_3 = z_3$, $q_4 = z_4$, $q_b = z_5$ in the expressions above; note in particular that z_2 is the series impedance of the source (for an ideal voltage source one has $z_2 = 0$). The transfer admittance is well-defined in this context and reads, from (29), as

$$\frac{i_5}{v_{s_1}} = \frac{-z_4}{z_4 z_5 + z_3 z_4 + z_2 z_5 + z_2 z_4 + z_2 z_3},$$

which corresponds to (2.200) in [4, p. 106] in the absence of coupling (set $z_0 = 0$ there).

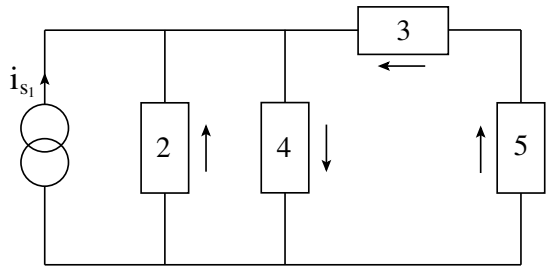


Figure 5: Describing the source as a current source.

Voltage- and current-controlled descriptions can be also combined. Assume e.g. that the source is described as a (possibly nonideal) current source, by fixing $p_a = y_2$, $q_a = 1$ (Figure 5; cf. Fig. 2.23 in [4, p. 94]). For the immittance at branch 3 we choose an impedance description, with $p_3 = 1$ and $q_3 = z_3$, whereas immittances 4 and 5 are described as admittances, with $p_4 = y_4$, $p_b = y_5$ and $q_4 = q_b = 1$. In this specific context, the transfer impedance is obtained from (30) and reads as

$$\frac{v_5}{i_{s_1}} = \frac{-1}{y_2 + y_2 z_3 y_5 + y_4 + y_5 + z_3 y_4 y_5}.$$

By setting $y_2 = 1/z_2$, this matches again the expression given in (2.201) in [4, p. 106] for the case $z_0 = 0$. Note that our approach yields both the transfer admittance and the transfer impedance by means of a single analysis; even if we do not carry out further details, the other two transfer functions are also obtained in the same manner (cf. (28) and (31)). Moreover, in all cases the corresponding expressions hold without the need to resort to specific admittance/impedance descriptions for the different circuit devices.

3.3 Further order reduction in the presence of voltage-controlled devices

The computation of transfer functions via Theorem 1 is feasible for almost completely arbitrary two-ports, the only restriction being the uncoupled nature assumed for the input and the output. However, in practice most circuit devices have an admittance description, and one may profit from this fact to further reduce the order of the matrices arising in (11), provided that such voltage-controlled devices are uncoupled from the remaining ones.

From the linear algebra standpoint, the key result is given in Lemma 2 below. Here, we are describing the set of voltage-controlled devices by the relation $i_y = Y v_y$, where Y is the corresponding branch-admittance matrix: we use the subscript y to refer to the set of voltage-controlled devices, whereas the remaining ones are labeled with a tilde ($\tilde{}$). Now the order is reduced from $m + n - 1$ (for the matrix in the left-hand side of (32)) to $\tilde{m} + n - 1$ (for the one in the right-hand side), where $\tilde{m}$ is the number of circuit elements which are not voltage-controlled. For simplicity, we assume that branches are ordered in a way such that the voltage-controlled devices are the first ones.

Lemma 2. *Assume* $A = \begin{pmatrix} A_y & \tilde{A} \end{pmatrix}$, $P = \text{block-diag}(Y, \tilde{P})$, $Q = \text{block-diag}(I, \tilde{Q})$. *Then*

$$\det \begin{pmatrix} 0 & A \\ -PA^{\mathsf{T}} & Q \end{pmatrix} = \det \begin{pmatrix} A_y Y A_y^{\mathsf{T}} & \tilde{A} \\ -\tilde{P}\tilde{A}^{\mathsf{T}} & \tilde{Q} \end{pmatrix}. \tag{32}$$

Proof. Just note that the block-diagonal structure of P and Q, reflecting the assumption that the set of voltage-controlled devices is uncoupled from the remaining ones, gives the matrix in the left-hand side of (32) the form

$$\begin{pmatrix} 0 & A \\ -PA^{\mathsf{T}} & Q \end{pmatrix} = \begin{pmatrix} 0 & A_y & \tilde{A} \\ -YA_y^{\mathsf{T}} & I & 0 \\ -\tilde{P}\tilde{A}^{\mathsf{T}} & 0 & \tilde{Q} \end{pmatrix}.$$

The claim then follows from a Schur reduction [13], using the identity block within the latter matrix. □

Our treatment of devices which are not assumed to be voltage-controlled is aimed at two different purposes: on the one hand, we want to accommodate in this group devices whose nature is left unspecified, at least up to a certain stage in the modeling process. In particular, this will apply to the input and the output of the two-ports considered throughout the paper: for the input port, namely branch j, we want to be able to accommodate, in the same analysis, both a voltage and a current source (either ideal or nonideal, in both cases), whereas for the output port (branch k) we want to be able to handle any load, including a short-circuit and an open-circuit. For this reason we are using homogeneous parameters $(p_j : q_j)$ and $(p_k : q_k)$ for the ports. On the other hand, we also want this group of devices to model circuit elements which do not have an admittance description; not only those described in impedance terms, but also those which do not admit either an admittance or an impedance description. Operational amplifiers, to be extensively discussed later, will provide a salient example of the latter case. Accordingly, we further split the group of devices which are not voltage-controlled into the ports, on the one hand, and the remaining ones (to be described with the subscript h, from "homogeneous"), on the other. Therefore, assuming again the appropriate branch ordering, we may write $\tilde{A} = \begin{pmatrix} A_j & A_k & A_h \end{pmatrix}$ and, from the assumption that the ports are uncoupled from the remaining devices, $\tilde{P} = \text{block-diag}(p_j, p_k, P_h)$, $\tilde{Q} = \text{block-diag}(q_j, q_k, Q_h)$.

Theorem 2. *Consider a two-port with input j and output k, both ports behaving as in Theorem 1, and assume that the remaining branches are split into two mutually uncoupled groups, one of them having an admittance description with branch-admittance matrix Y, whereas for the other group we use a homogeneous description with matrices P_h, Q_h. Then, the determinants (11) can be computed as*

$$\eta = \det \begin{pmatrix} A_y Y A_y^{\mathsf{T}} & A_j & A_h \\ -A_k^{\mathsf{T}} & 0 & 0 \\ -P_h A_h^{\mathsf{T}} & 0 & Q_h \end{pmatrix}, \quad \zeta = \det \begin{pmatrix} A_y Y A_y^{\mathsf{T}} & A_j & A_k & A_h \\ -p_j A_j^{\mathsf{T}} & q_j & 0 & 0 \\ -p_k A_k^{\mathsf{T}} & 0 & q_k & 0 \\ -P_h A_h^{\mathsf{T}} & 0 & 0 & Q_h \end{pmatrix}. \tag{33}$$

Proof. The key idea is the one used in Lemma 2. As in the proof of Theorem 1, the expression given for η in (11) is easily seen equivalent to

$$\det \begin{pmatrix} 0 & A_j & A_k & A_r \\ -A_k^{\mathsf{T}} & 0 & 0 & 0 \\ 0 & 0 & 1 & 0 \\ -P_r A_r^{\mathsf{T}} & 0 & 0 & Q_r \end{pmatrix}.$$

There is no loss of generality in assuming that branches are ordered in a way such that $A_r = \begin{pmatrix} A_y & A_h \end{pmatrix}$, $P_r = \text{block-diag}(Y, P_h)$, $Q_r = \text{block-diag}(I, Q_h)$. Now, an even permutation of rows and columns gives the above determinant the form

$$\det \begin{pmatrix} 0 & A_y & A_j & A_k & A_h \\ -YA_y^\mathsf{T} & I & 0 & 0 & 0 \\ -A_k^\mathsf{T} & 0 & 0 & 0 & 0 \\ 0 & 0 & 0 & 1 & 0 \\ -P_h A_h^\mathsf{T} & 0 & 0 & 0 & Q_h \end{pmatrix}.$$

This has the form depicted in the left-hand side of (32), with $A = \begin{pmatrix} A_y & \tilde{A} \end{pmatrix}$, $\tilde{A} = \begin{pmatrix} A_j & A_k & A_h \end{pmatrix}$ and

$$P = \begin{pmatrix} Y & 0 & 0 & 0 \\ 0 & 0 & 1 & 0 \\ 0 & 0 & 0 & 0 \\ 0 & 0 & 0 & P_h \end{pmatrix}, \quad Q = \begin{pmatrix} I & 0 & 0 & 0 \\ 0 & 0 & 0 & 0 \\ 0 & 0 & 1 & 0 \\ 0 & 0 & 0 & Q_h \end{pmatrix}.$$

The determinant in the right-hand side of (32) turns out to be in this case

$$\begin{pmatrix} A_y Y A_y^\mathsf{T} & A_j & A_k & A_h \\ -A_k^\mathsf{T} & 0 & 0 & 0 \\ 0 & 0 & 1 & 0 \\ -P_h A_h^\mathsf{T} & 0 & 0 & Q_h \end{pmatrix},$$

and the equivalent expression given to η in (33) readily follows. For ζ, we proceed in the same manner: with the same permutation of rows and columns and by setting

$$P = \begin{pmatrix} Y & 0 & 0 & 0 \\ 0 & p_j & 0 & 0 \\ 0 & 0 & p_k & 0 \\ 0 & 0 & 0 & P_h \end{pmatrix}, \quad Q = \begin{pmatrix} I & 0 & 0 & 0 \\ 0 & q_j & 0 & 0 \\ 0 & 0 & q_k & 0 \\ 0 & 0 & 0 & Q_h \end{pmatrix},$$

the expression given in (33) follows from the form that the determinant in the right-hand side of (32) takes in this case. □

The expressions given in (33) allow for an efficient computation of all four transfer functions of a really broad family of two-ports (specifically, those meeting the assumptions of Theorem 2) using the formulae (12). For practical purposes, it is also of interest to particularize such expressions to circuits in which the source at the input is an ideal one and the output amounts either to an open-circuit or to a short-circuit. This is easily modeled by setting the values of the parameters p_j, q_j, p_k and q_k either to 1 or to 0, as detailed below. In all such cases, the corresponding transfer function amounts to the quotient η/ζ, where η is not dependent on the terminations (note that p_j, q_j, p_k and q_k do not enter the determinant defining η in (33)). The different expressions for the denominator ζ are given in what follows; we use the subscripts v, y, etc. to make it explicit that the determinant is the one defining the voltage gain, the transfer admittance, etc.

Note first that an ideal voltage source at branch j is modeled by the parameter values $p_j = 1$, $q_j = 0$. In this context, the open-circuit voltage gain v_k/v_{s_j} is obtained with $p_k = 0$, $q_k = 1$, and the denominator arising in this transfer function amounts to

$$\zeta_v = \det \begin{pmatrix} A_y Y A_y^\mathsf{T} & A_j & A_h \\ -A_j^\mathsf{T} & 0 & 0 \\ -P_h A_h^\mathsf{T} & 0 & Q_h \end{pmatrix}. \tag{34}$$

Similarly, the short-circuit transfer admittance is modeled by the parameter values $p_k = 1$, $q_k = 0$, and the denominator is now

$$\zeta_y = \det \begin{pmatrix} A_y Y A_y^\mathsf{T} & A_j & A_k & A_h \\ -A_j^\mathsf{T} & 0 & 0 & 0 \\ -A_k^\mathsf{T} & 0 & 0 & 0 \\ -P_h A_h^\mathsf{T} & 0 & 0 & Q_h \end{pmatrix}. \tag{35}$$

The other two cases involve an ideal current source at the input, obtained with the values $p_j = 0$, $q_j = 1$. The open-circuit transfer impedance requires setting $p_k = 0$, $q_k = 1$, and in this case the denominator of the transfer function can be simply written as

$$\zeta_z = \det \begin{pmatrix} A_y Y A_y^\mathsf{T} & A_h \\ -P_h A_h^\mathsf{T} & Q_h \end{pmatrix}. \tag{36}$$

Finally, for the short-circuit current gain one sets $p_k = 1$, $q_k = 0$, and the corresponding denominator amounts to

$$\zeta_i = \det \begin{pmatrix} A_y Y A_y^\mathsf{T} & A_k & A_h \\ -A_k^\mathsf{T} & 0 & 0 \\ -P_h A_h^\mathsf{T} & 0 & Q_h \end{pmatrix}. \tag{37}$$

We will exploit the formula (34) for the voltage gain in Section 4, and the reader is referred to that section for a comprehensive discussion of examples. However, worth emphasizing at this point is the fact that all other transfer functions can be computed in completely analogous terms, as detailed above.

3.4 Classical cofactors formulae and Chen's generalized cofactors

Cofactors formulae, either in a classical context but also in the generalized setting of [4, 5], can be derived from the results above, as detailed in this section. We begin by deriving Chen's generalized cofactors formulae, since classical formulae can be obtained as a particular case.

Generalized cofactors formulae. Let us focus on the problem of finding the transfer impedance v_k/i_{s_j} of a given two-port. To do so, in [4, Section 4.5] the author assumes that all internal devices can be given an admittance description. As detailed in previous sections, this would be an unnecessarily restrictive assumption in our framework, but for the sake of comparison let us work in this scenario. This transfer function is defined by the ratio η/ζ_z, and the numerator and denominator amount in this setup to

$$\eta = \det \begin{pmatrix} A_y Y A_y^\mathsf{T} & A_j \\ -A_k^\mathsf{T} & 0 \end{pmatrix} \tag{38}$$

and $\zeta_z = \det\left(A_y Y A_y^{\mathsf{T}}\right)$: these expressions come from (33) and (36), respectively, in the absence of the homogeneous blocks. Recall that A is an arbitrary reduced cutset matrix or a reduced incidence matrix. In (38) we may perform a Laplace expansion along the last column and then along the last row to obtain

$$\begin{aligned}\det\begin{pmatrix} A_y Y A_y^{\mathsf{T}} & A_j \\ -A_k^{\mathsf{T}} & 0 \end{pmatrix} &= -\det\begin{pmatrix} A_y Y A_y^{\mathsf{T}} & A_j \\ A_k^{\mathsf{T}} & 0 \end{pmatrix} = -\sum_{i_1=1}^{n-1}(-1)^{i_1+n} a_{i_1 j} \det\begin{pmatrix} A_{y[-i_1]} Y A_y^{\mathsf{T}} \\ A_k^{\mathsf{T}} \end{pmatrix} \\ &= -\sum_{i_1=1}^{n-1}(-1)^{i_1+n} a_{i_1 j}\left[\sum_{i_2=1}^{n-1} a_{i_2 k}(-1)^{n-1+i_2} \det\left(A_{y[-i_1]} Y A_{y[-i_2]}^{\mathsf{T}}\right)\right] \\ &= \sum_{i_1=1}^{n-1}\sum_{i_2=1}^{n-1}(-1)^{i_1+i_2} a_{i_1 j} a_{i_2 k} \det\left(A_{y[-i_1]} Y A_{y[-i_2]}^{\mathsf{T}}\right), \end{aligned} \tag{39}$$

where $A_y[-i_x]$ stands for the submatrix of A_y obtained after removing the i_x-th row. This expression is the generalized cofactor as defined in (2.170b) of [4], and our quotient η/ζ_z accounts for the expression given later in (2.191) (notice the negative sign in Chen's book, owing to the different convention for the reference directions). Let us emphasize that the derivation above is rather straightforward; actually, we believe it simpler to use directly a determinant such as (38) rather than the formula (39) resulting from the expansion.

Classical cofactors formulae. Examples such as the one discussed in the Introduction also arise as particular cases of the formulae obtained above. Note that for notational simplicity we used there A for what is now A_y, that is, the reduced incidence matrix once the input and output ports are removed (the input and output ports in the example in the Introduction would be oriented from nodes α and β, respectively, towards the reference node, and note that the output there is an open-circuit). The only nonzero entries within A_j and A_k would be $a_{\alpha j} = 1$ and $a_{\beta k} = 1$, respectively. The expression given to η in (39) then amounts to

$$(-1)^{\alpha+\beta} \det\left(A_{y[-\alpha]} Y A_{y[-\beta]}^{\mathsf{T}}\right),$$

which is indeed the cofactor of the (α, β)-entry of the node-admittance matrix (to be written as $\Delta_{\alpha,\beta}$ in the sequel). Note also that the denominator (Δ in (2) in the Introduction) is given as well by our expression for ζ_z in (36), which in this setup simply reads as $\det\left(A_y Y A_y^{\mathsf{T}}\right)$.

The assumption that the input and the output are incident with the reference node can be easily removed. Assume for instance that the output is directed from node β to node γ. This yields $a_{\gamma k} = -1$, and therefore

$$\eta = \Delta_{\alpha,\beta} - \Delta_{\alpha,\gamma},$$

according to (39) (compare e.g. with (2.20) in [21, p. 164]). Likewise, if the input branch is directed from node α to node ω, we get $a_{\omega,j} = -1$ and then

$$\eta = \Delta_{\alpha,\beta} - \Delta_{\alpha,\gamma} - \Delta_{\omega,\beta} + \Delta_{\omega,\gamma},$$

using again (39).

To sum up, the results stated in Theorems 1 and 2 cover in particular the classical and generalized cofactors formulae for the transfer impedance; such formulae can be easily derived

as corollaries of the aforementioned results, as detailed above. Other transfer functions, which become increasingly complex when addressed via classical methods (for comparison, see [5]), can be treated in our framework in the same manner, using in these cases the denominators provided by ζ_v, ζ_y and ζ_i in (34), (35) and (37), and without the need to assume that all internal devices are given an admittance description. For these reasons, we believe our approach to have a theoretical value as a comprehensive framework to accommodate this type of results. It should also be of interest for practical purposes, as discussed in the next section.

4 Application to the symbolic analysis of active filters

We apply in this section some of the results above to the analysis of active filters, focusing on the role that the parameters arising in nonideal models of the operational amplifiers have on the voltage gain of the different filters. The goal is to show that our analytical framework makes it possible to address certain problems which are not easily tackled with conventional techniques. We focus on a specific problem, namely the location of the peak frequency of the voltage gain. The reason to do so is mainly illustrative; the point is that this peak frequency is computed analytically, and addressing its sensitivity to certain parameters requires implicit differentiation techniques which are feasible because an explicit expression for the transfer function is available. Of course, the techniques here presented should be of interest in other problems involving active filters and also in the analysis of other circuits including op-amps.

4.1 VCVS filter

Figure 6 displays a VCVS filter (the name is taken from [14, p. 407]; see also [9, 15, 20]). Note that we use a generic admittance description for branches 1-4; different assignments of capacitors and resistors to Y_1 through Y_4 are well-known to yield lowpass, high-pass and band-pass circuits. We formulate the model in terms of abstract admittances, without resorting to such particular setups, for the sake of generality in what follows.

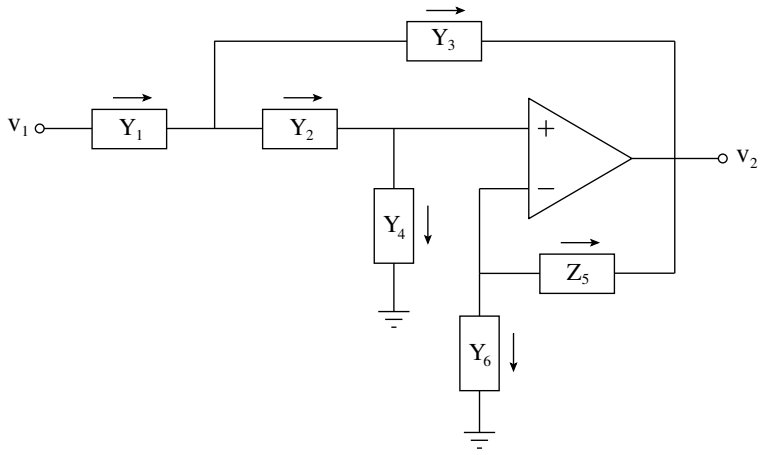


Figure 6: VCVS filter.

The op-amp, together with branches 5-6, sets up a noninverting amplifier configuration. In practice, branches 5 and 6 accommodate two resistors, to be described in terms of their

resistance R_5 and conductance G_6, respectively. The (ideal) closed-loop gain of the noninverting amplifier turns out to be $k = 1 + R_5 G_6$. We choose the above descriptions to account easily for the particular case given by the values $R_5 = 0$ and $G_6 = 0$: the whole analysis carried out below for the VCVS filter will apply to this particular case, in which the op-amp just behaves as a voltage follower and therefore $k = 1$. With the values $R_5 = 0$, $G_6 = 0$ we get the Sallen-Key filter; again, we borrow the terminology from [14, p. 399] and reserve the Sallen-Key label for the unity gain case, although worth mentioning is that the Sallen-Key and VCVS designations are often used interchangeably for the filter in Figure 6.

We are interested in computing symbolically the voltage gain v_2/v_1. This is given by the quotient η/ζ_v, with η and ζ_v defined in (33) and (34), respectively. With regard to the expressions given there, note that when some of the devices which are not voltage-controlled admit an impedance description (and are uncoupled from the remaining ones), we may bring them out of the homogeneous blocks, to obtain

$$\eta = \det \begin{pmatrix} A_y Y A_y^\mathsf{T} & A_j & A_z & A_h \\ -A_k^\mathsf{T} & 0 & 0 & 0 \\ -A_z^\mathsf{T} & 0 & Z & 0 \\ -P_h A_h^\mathsf{T} & 0 & 0 & Q_h \end{pmatrix}, \ \zeta_v = \det \begin{pmatrix} A_y Y A_y^\mathsf{T} & A_j & A_z & A_h \\ -A_j^\mathsf{T} & 0 & 0 & 0 \\ -A_z^\mathsf{T} & 0 & Z & 0 \\ -P_h A_h^\mathsf{T} & 0 & 0 & Q_h \end{pmatrix}, \tag{40}$$

where z is the subscript used to specify such devices and Z is the corresponding impedance matrix. Notice that the blocks labeled with the subscript h are now assumed to exclude the set of devices with an impedance description. As in previous sections, the subindices j and k are used to denote generically the input and output branches.

In the VCVS filter, the impedance matrix has a single entry defined by the R_5 parameter, whereas the homogeneous block is defined by the op-amp in the terms detailed in Section 2.1 (the corresponding blocks can be found in (8)). For the definition of the reduced incidence matrix, we number the nodes in Figure 6 as follows: node 1 is the input node, node 2 is the one in between Y_1 and Y_2, nodes 3 and 4 are the noninverting and inverting input terminals of the op-amp, whereas node 5 is the output node. Together with the reference directions displayed in the figure, this yields

$$A_y = \begin{pmatrix} 1 & 0 & 0 & 0 & 0 \\ -1 & 1 & 1 & 0 & 0 \\ 0 & -1 & 0 & 1 & 0 \\ 0 & 0 & 0 & 0 & 1 \\ 0 & 0 & -1 & 0 & 0 \end{pmatrix}, \ A_z = \begin{pmatrix} 0 \\ 0 \\ 0 \\ 1 \\ -1 \end{pmatrix}, \ A_h = \begin{pmatrix} 0 & 0 \\ 0 & 0 \\ 1 & 0 \\ -1 & 0 \\ 0 & 1 \end{pmatrix}. \tag{41}$$

Finally, the column incidence matrices of the input and output branches are $\begin{pmatrix} 1 & 0 & 0 & 0 & 0 \end{pmatrix}^\mathsf{T}$ and $\begin{pmatrix} 0 & 0 & 0 & 0 & 1 \end{pmatrix}^\mathsf{T}$, respectively. This way, the determinants (40), defining the transfer

function η/ζ_v, turn out to be

$$\eta = \det \begin{pmatrix} y_1 & -y_1 & 0 & 0 & 0 & 1 & 0 & 0 & 0 \\ -y_1 & y_1+y_2+y_3 & -y_2 & 0 & -y_3 & 0 & 0 & 0 & 0 \\ 0 & -y_2 & y_2+y_4 & 0 & 0 & 0 & 0 & 1 & 0 \\ 0 & 0 & 0 & G_6 & 0 & 0 & 1 & -1 & 0 \\ 0 & -y_3 & 0 & 0 & y_3 & 0 & -1 & 0 & 1 \\ 0 & 0 & 0 & 0 & -1 & 0 & 0 & 0 & 0 \\ 0 & 0 & 0 & -1 & 1 & 0 & R_5 & 0 & 0 \\ 0 & 0 & -G_i & G_i & 0 & 0 & 0 & 1 & 0 \\ 0 & 0 & 1 & -1 & -b & 0 & 0 & 0 & bR_0 \end{pmatrix} \tag{42}$$

and

$$\zeta_v = \det \begin{pmatrix} y_1 & -y_1 & 0 & 0 & 0 & 1 & 0 & 0 & 0 \\ -y_1 & y_1+y_2+y_3 & -y_2 & 0 & -y_3 & 0 & 0 & 0 & 0 \\ 0 & -y_2 & y_2+y_4 & 0 & 0 & 0 & 0 & 1 & 0 \\ 0 & 0 & 0 & G_6 & 0 & 0 & 1 & -1 & 0 \\ 0 & -y_3 & 0 & 0 & y_3 & 0 & -1 & 0 & 1 \\ -1 & 0 & 0 & 0 & 0 & 0 & 0 & 0 & 0 \\ 0 & 0 & 0 & -1 & 1 & 0 & R_5 & 0 & 0 \\ 0 & 0 & -G_i & G_i & 0 & 0 & 0 & 1 & 0 \\ 0 & 0 & 1 & -1 & -b & 0 & 0 & 0 & bR_0 \end{pmatrix}, \tag{43}$$

respectively. Explicitly, these functions read, in terms of the parameter $k = 1 + R_5G_6$, as

$$\eta = y_1[ky_2 + bR_0[k(y_2y_3 + y_3y_4) + G_i(y_2 + ky_3 + R_5(y_2y_3 + y_3y_4))]] \tag{44}$$

and

$$\begin{aligned} \zeta_v =& y_1y_2 + y_1y_4 + y_2y_4 + y_3y_4 - R_5G_6y_2y_3 + b[k[y_1y_2 + y_1y_4 + y_2y_3 + y_2y_4 + y_3y_4] \\ &+ R_0[k(y_1y_2y_3 + y_1y_3y_4 + y_2y_3y_4) + G_6(y_1y_2 + y_1y_4 + y_2y_3 + y_2y_4 + y_3y_4)] \\ &+ G_i[k(y_1 + y_2 + y_3) + R_5(y_1y_2 + y_1y_4 + y_2y_3 + y_2y_4 + y_3y_4)] \\ &+ R_0G_i[y_1y_2 + y_1y_3 + y_1y_4 + y_2y_4 + y_3y_4 + R_5(y_1y_2y_3 + y_1y_3y_4 + y_2y_3y_4) \\ &+ G_6(y_1 + y_2 + y_3) + R_5G_6(y_1y_3 + y_2y_3)]]. \end{aligned} \tag{45}$$

Needless to say, the three parameters that accommodate nonidealities in the op-amp (viz., the inverse of the gain, b, the input conductance, G_i, and the output resistance, R_0) appear explicitly in the expressions above. By annihilating b, G_i and R_0 one gets the expressions for the numerator and the denominator of the voltage gain when using an ideal op-amp, namely

$$\eta = ky_1y_2, \quad \zeta_v = y_1y_2 + y_1y_4 + y_2y_4 + y_3y_4 - R_5G_6y_2y_3.$$

We emphasize the generality of the approach above. This is in contrast to the use of *ad-hoc* techniques such as the ones involving voltage-constrained terminals detailed in Chen's book [5] (pp. 117-126). Also, in our framework there is no need to make a separate treatment of the ideal and nonideal cases for the op-amps (compare again with [5, pp. 127-131]). Just

for the sake of comparison, a lowpass VCVS filter is obtained by letting Y_1 and Y_2 be resistors and Y_3 and Y_4 capacitors in Figure 6. We just need to set $y_1 = G_1$, $y_2 = G_2$, $y_3 = sC_1$ and $y_4 = sC_2$ in the expressions above in order to accommodate this setup. Specifically, finite gain is the only nonideality considered in Chen's analysis of the VCVS filter; by performing the substitutions indicated above together with $G_i = 0$, $R_0 = 0$, one readily gets from (44) and (45) the transfer function

$$\frac{\eta}{\zeta_v} = \frac{kG_1G_2}{(1+bk)(G_1G_2 + s(G_1+G_2)C_2 + sG_2C_1 + s^2C_1C_2) - skG_2C_1}, \tag{46}$$

as in [5, eq. (2.160)].

We may, however, exploit expressions such as the ones depicted in (44) and (45) in much broader contexts. As a sample of the analyses allowed by our symbolic framework, we perform in what follows a detailed analysis of the frequency response of different filters with realistic models of the op-amp, that is, taking into account the fact that both the input conductance and the output resistance may not vanish, and also that the open-loop gain may be finite and also depend on the frequency, as detailed below.

4.2 Frequency response

Let us focus on the low pass configuration of the VCVS filter and work in terms of the real frequency $f = \omega/(2\pi)$ by setting $y_1 = G_1$, $y_2 = G_2$, $y_3 = j\omega C_1$ and $y_4 = j\omega C_2$ in the expressions (44)-(45) obtained above. Allowing G_i and R_0 to take nonzero values, our aim is to examine the frequency response of the filter not only for a constant, finite gain in the op-amp but also for a frequency-dependent one. In the latter context, we want to exploit the analytical framework discussed above to examine how the location of the peak frequency depends on the G_i and R_0 parameters of the op-amp. This is just an example of the analyses that are feasible in our symbolic framework. Worth noting is that such an analysis cannot be carried out with conventional numerical tools such as the ones available in most circuit simulators. Details follow.

Sallen-Key filter. For simplicity, let us begin with the Sallen-Key filter (Figure 7), by assuming $R_5 = G_6 = 0$ in the analysis above; hence $k = 1$.

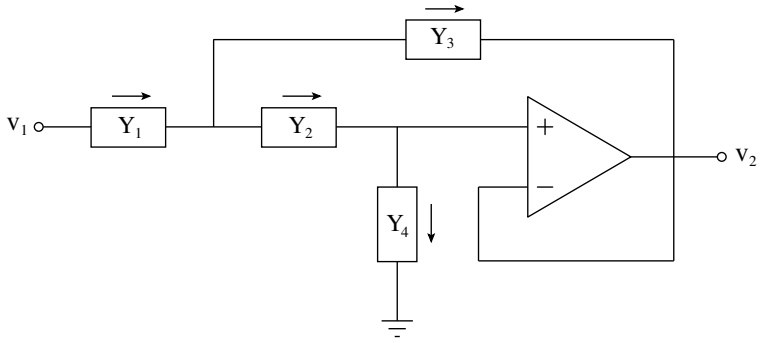


Figure 7: Sallen-Key filter.

In this setting, (44) and (45) yield

$$\eta = y_1[y_2 + bR_0[y_2y_3 + y_3y_4 + G_i(y_2 + y_3)]], \tag{47}$$

and

$$\begin{aligned}\zeta_v =& y_1y_2 + y_1y_4 + y_2y_4 + y_3y_4 + b[y_1y_2 + y_1y_4 + y_2y_3 + y_2y_4 + y_3y_4 + R_0(y_1y_2y_3 + y_1y_3y_4 \\ &+ y_2y_3y_4) + G_i(y_1 + y_2 + y_3) + R_0G_i(y_1y_2 + y_1y_3 + y_1y_4 + y_2y_4 + y_3y_4)],\end{aligned} \tag{48}$$

with $\eta = y_1y_2$ and $\zeta_v = y_1y_2 + y_1y_4 + y_2y_4 + y_3y_4$ when using an ideal op-amp.

Assume first that the op-amp has a constant, finite gain a. For later comparison, set $a = 10^5$, and therefore $b = a^{-1} = 10^{-5}$. For the discrete components we use $R_1 = 5.76$ kΩ, $R_2 = 2.21$ kΩ (and, accordingly, $y_1 = 1/R_1$, $y_2 = 1/R_2$), $C_1 = 20$ nF, $C_2 = 1$ nF (with $y_3 = j\omega C_1$, $y_4 = j\omega C_2$). These values are borrowed from [9, pp. 145-146]. For the parameters G_i and R_0 we use two sets of values: with $G_i = 0$ S, $R_0 = 0$ Ω we get $f_{\max} = 9331.571$ Hz (Figure 8). In this constant-gain setup, the nonideal values $G_i = 10^{-6}$ S, $R_0 = 100$ Ω only yield a small change in the location of the maximum, which is found at $f_{\max} = 9331.565$ Hz.

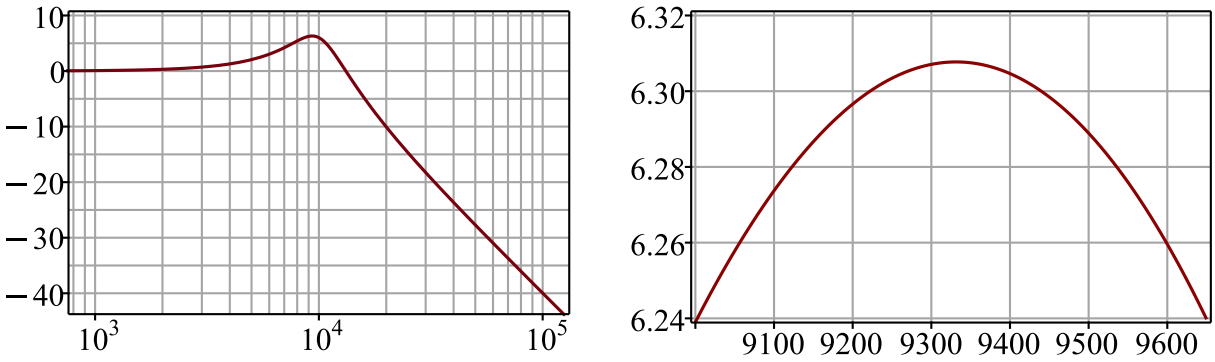


Figure 8: Constant open-loop gain in the Sallen-Key filter. (a) Left: frequency response. (b) Right: detail near the peak frequency (with the frequency plotted on a linear scale).

The location of the peak frequency turns out to be more sensitive to these parameters when using a frequency-dependent model for the open-loop gain. Consider a gain described by the single-pole model $a(f) = a_0/(1 + jf/f_b)$, with $a_0 = 10^5$, $f_b = 10$ Hz, as in [9, pp. 280-281]. Accordingly, we write $b(f) = b_0(1 + jf/f_b)$, with $b_0 = 10^{-5}$. Now, when both G_i and R_0 are assumed to vanish the peak is met at $f_{\max} = 9052.887$ Hz (Figure 9). Mind the different location of the peak frequency with respect to the constant gain setup considered above.

In this single-pole scenario, the values $G_i = 10^{-6}$ S, $R_0 = 100$ Ω yield $f_{\max} = 9048.599$ Hz; that is, a shift of more than 4 hertz results from the use of such nonideal values for the op-amp parameters. For illustration, the location of the peak frequencies for $G_i = 0$ S, $R_0 = 0$ Ω and $G_i = 10^{-6}$ S, $R_0 = 100$ Ω are depicted in Figure 10.

The results reported up to this point can be also obtained with conventional simulators. But a more accurate analysis of the dependence of the peak frequency on the parameters G_i

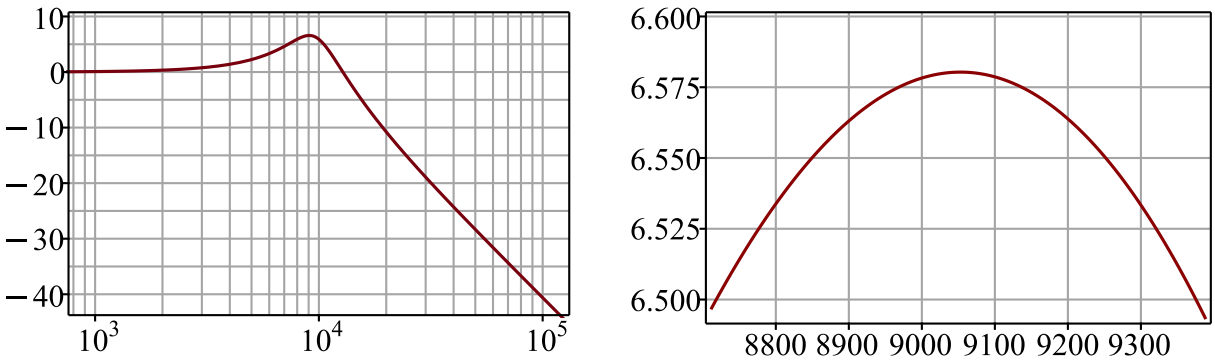


Figure 9: Single-pole model for the open-loop gain in the Sallen-Key filter, with $G_i = R_0 = 0$. (a) Left: frequency response. (b) Right: detail near the peak frequency.

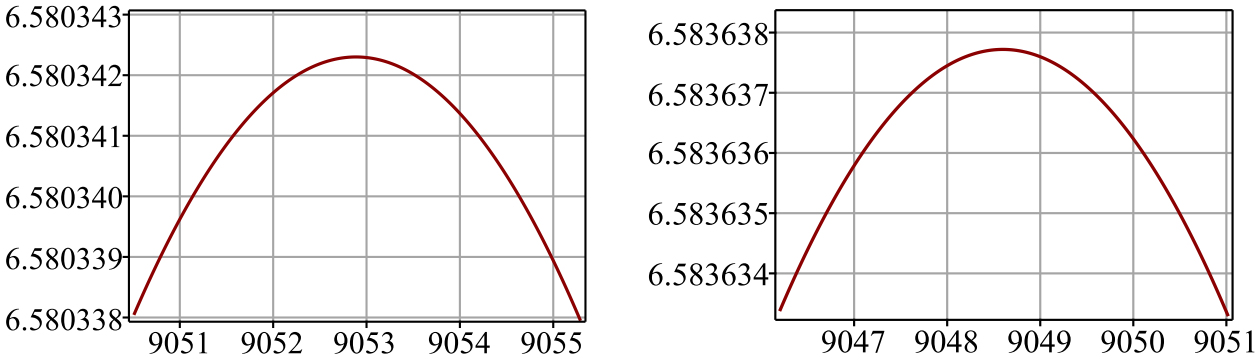


Figure 10: Peak frequency shift (single-pole). (a) $G_i = R_0 = 0$. (b) $G_i = 10^{-6}$, $R_0 = 100$.

and R_0 is feasible in our framework. This is just an example of an analysis which is made possible by the availability of a symbolic expression for the transfer function in terms of all circuit parameters. Worth emphasizing is that, in all what follows, results are exact except for round-off errors.

Indeed, the deviation in the peak frequency observed in the single-pole open-loop gain scenario can be explained in analytical terms as follows. Let $T(f, G_i, R_0)$ stand for the modulus $|\eta/\zeta_v|$, written as a function of f, G_i and R_0 and with the values detailed above for all the remaining parameters in (47) and (48). Moreover, let $h(f, G_i, R_0) = 0$ describe implicitly the location of the peak frequency; in light of the data above we have, for instance, $h(9052.887, 0, 0) = 0$, $h(9048.599, 10^{-6}, 100) = 0$, ignoring round-off errors. By solving for f in $h(f, G_i, R_0) = 0$ we may write the peak frequency $f_{\max}$ as a function $\tilde{h}(G_i, R_0)$ of the op-amp parameters G_i and R_0. Additionally, the partial derivatives $\partial\tilde{h}/\partial G_i$ and $\partial\tilde{h}/\partial R_0$ can be obtained by implicit differentiation, namely as

$$\frac{\partial\tilde{h}}{\partial G_i} = -\frac{\partial h/\partial G_i}{\partial h/\partial f} = -\frac{\partial^2 T/\partial f \partial G_i}{\partial^2 T/\partial f^2}, \quad \frac{\partial\tilde{h}}{\partial R_0} = -\frac{\partial h/\partial R_0}{\partial h/\partial f} = -\frac{\partial^2 T/\partial f \partial R_0}{\partial^2 T/\partial f^2}.$$

Here we have made use of the fact that the function h just amounts to the partial derivative $\partial T/\partial f$, since the peak frequency is a critical point of T considered as a function of f (that is, for fixed values of G_i and R_0). Actually, the peak frequencies reported above have been computed by finding the zeros of the derivative $\partial T/\partial f$.

Now, all the partial derivatives arising above can be explicitly computed because an analytical expression for T is available in our framework. By letting $f^0_{\max}$ stand for the peak frequency 9052.887 for $G_i = R_0 = 0$, we get

$$\frac{\partial \tilde{h}}{\partial G_i}(0,0) = -\left.\frac{\partial^2 T/\partial f \partial G_i}{\partial^2 T/\partial f^2}\right|_{f=f^0_{\max},G_i=0,R_0=0} = -\left(\frac{-0.286901}{-3.696601\cdot 10^{-7}}\right) = -776121.03$$

and

$$\frac{\partial \tilde{h}}{\partial R_0}(0,0) = -\left.\frac{\partial^2 T/\partial f \partial R_0}{\partial^2 T/\partial f^2}\right|_{f=f^0_{\max},G_i=0,R_0=0} = -\left(\frac{-1.293698\cdot 10^{-8}}{-3.696601\cdot 10^{-7}}\right) = -0.034997.$$

The linear approximation of $\tilde{h}$ near the origin is

$$\tilde{h}(G_i, R_0) \approx f^0_{\max} + \frac{\partial \tilde{h}}{\partial G_i}(0,0)G_i + \frac{\partial \tilde{h}}{\partial R_0}(0,0)R_0,$$

which provides an estimation $f_{\max} \approx 9052.887 - 776121.03\cdot 10^{-6} - 0.034997\cdot 100 = 9048.611$ Hz for $G_i = 10^{-6}$ S, $R_0 = 100\ \Omega$. This is an excellent approximation of the actual value 9048.599 obtained above. Looking at the effect of the nonideal nature of both parameters, the output resistance R_0 turns out to be more relevant than the input conductance G_i with regard to the location of the peak frequency.

VCVS filter. The same analysis can be performed for the VCVS filter of Figure 6. We borrow from [9, pp. 144-145] the parameter values $R_1 = R_2 = 15.8$ kΩ, (with $y_1 = 1/R_1$, $y_2 = 1/R_2$), $C_1 = C_2 = 10$ nF (and, again, $y_3 = j\omega C_1$, $y_4 = j\omega C_2$), $R_5 = 17.8$ kΩ, $G_6 = 10^{-4}$ S. For the open-loop gain we use again the single-pole model $a(f) = a_0/(1 + jf/f_b)$, with the parameter values $a_0 = 10^5$ and $f_b = 10$, yielding $b(f) = b_0(1 + jf/f_b)$, with $b_0 = 10^{-5}$.

With these numerical values, the peak frequency is located at $f_{\max} = 991.2778$ Hz when $G_i = R_0 = 0$. The values $G_i = 10^{-6}$ S, $R_0 = 100\ \Omega$ yield $f_{\max} = 991.2080$ Hz. Note that the deviation is much smaller than for the Sallen-Key filter with a single-pole model for the gain. This can be explained by computing the derivatives $\partial\tilde{h}/\partial G_i$ and $\partial\tilde{h}/\partial R_0$ for $G_i = R_0 = 0$ using implicit differentiation, as above. Details are entirely analogous to the ones above and are omitted for the sake of brevity. With $G_i = R_0 = 0$, the partial derivatives turn out to be $\partial\tilde{h}/\partial G_i = -54571.41$ and $\partial\tilde{h}/\partial R_0 = -0.0001478$. Both derivatives are much smaller than the ones obtained for the Sallen-Key filter, showing that the location of the peak frequency is much less sensitive to the op-amp parameters G_i, R_0. These derivatives account very accurately for the deviation reported above, since the linear approximation provides an estimation $f_{\max} \approx 991.2084$. Note that, in this case, the peak frequency is a bit more sensitive to the parameter G_i than to R_0.

4.3 Noninverting Kerwin-Huelsman-Newcomb filter

The same type of analysis is feasible for higher-scale circuits. We illustrate this in the present section by examining the noninverting Kerwin-Huelsman-Newcomb (KHN) filter depicted in

Figure 11. The branches labeled as Y_1 and Y_2 accommodate two capacitors, and we use a conductance description for all six resistors (G_1 through G_6 in the figure) to simplify matters. This filter is well-known to provide simultaneous highpass, bandpass and lowpass outputs ($v_{\rm HP}$, $v_{\rm BP}$ and $v_{\rm LP}$ in the figure) from a given input v_1. We refer the reader e.g. to [9, 14, 20] for detailed analyses of state-variable filters such as the KHN filter. The branches in Figure 11 are numbered as in [5, p. 132].

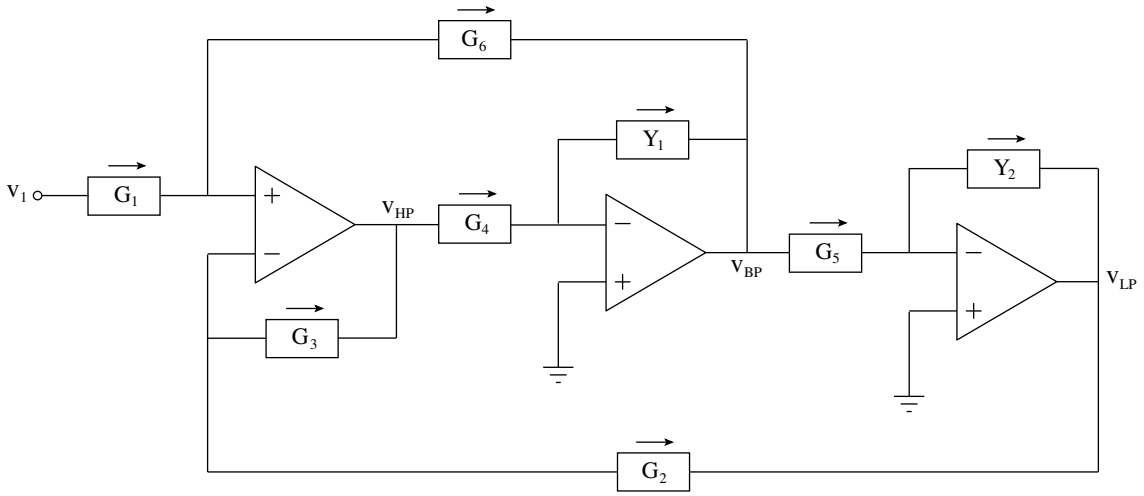


Figure 11: Noninverting Kerwin-Huelsman-Newcomb filter.

All three transfer functions can be computed exactly as detailed for the VCVS filter in Section 4.1. For the sake of brevity we just focus on the lowpass output. Assuming a constant, finite gain a (with inverse $b = a^{-1}$) for all three operational amplifiers, and also common symbolic parameters G_i and R_0 for the three op-amps, the lowpass transfer function involves 11 parameters and turns out to have 165 terms in the numerator and 856 in the denominator. There is no point in writing down here both expressions (as we did for the VCVS filter in (44) and (45)), but they can be found in the auxiliary data file Noninv-KHN-LowPass-Transfer-1.txt. In particular, by replacing in the aforementioned expression the ideal op-amp values $b = G_i = R_0 = 0$, one gets

$$\frac{v_{\rm LP}}{v_1} = \frac{G_1 G_4 G_5 (G_2 + G_3)}{(G_1 + G_6) G_2 G_4 G_5 + (G_2 + G_3) G_4 G_6 y_2 + (G_1 + G_6) G_3 y_1 y_2},$$

as in [5, eq. (2.172c)].

By using independent parameters b_k, G_{ik} and R_{0k} for all three op-amps ($k = 1$ stands for the summing amplifier and $k = 2$ and $k = 3$ for the two integrators, from left to right), the transfer function now involves 17 parameters and has 184 terms in the numerator and 1556 in the denominator. This transfer function can be found in the auxiliary data file Noninv-KHN-LowPass-Transfer-2.txt.

Along the lines of the above discussion of the Sallen-Key and VCVS filters, we may exploit these analytical expressions to address again the dependence of the peak frequency on the different parameters G_{ik} and R_{0k} of the three op-amps, provided that a common single-pole

model is used for the open-loop gain of all three amplifiers. Therefore we set b_1, b_2 and b_3 equal to $b_0(1 + jf/f_b)$, with $b_0 = 10^{-5}$ and $f_b = 10$ Hz. For the discrete components we borrow the following values from [18, Fig. 4]: $G_1 = G_2 = G_3 = 1/R_a$, $G_4 = G_5 = 1/R_b$ and $G_6 = 1/R_c$, with $R_a = 10$ kΩ, $R_b = 15.9$ kΩ and $R_c = 30$ kΩ, respectively, and, for the capacitors, $C_1 = C_2 = 1$ nF, with $y_k = j\omega C_k$ $(k = 1, 2)$.

When using the ideal values $G_i = 0$ S and $R_0 = 0$ Ω for all three op-amps, the peak frequency is located at $f_{\max} = 9428.4244$ Hz, whereas the values $G_{ik} = 10^{-6}$ S and $R_{0k} = 100$ Ω for $k = 1$, 2, 3 drive the peak frequency to $f_{\max} = 9429.9679$ Hz. However, the relative contribution of each individual parameter G_{ik} and R_{0k} remains somewhat hidden in these data. More detailed information can be found by computing the different sensitivities, using implicit differentiation as in previous cases. The different partial derivatives at the origin turn out to be

$$\frac{\partial \tilde{h}}{\partial G_{i1}} = 1.0878 \cdot 10^{6},\ \frac{\partial \tilde{h}}{\partial G_{i2}} = -0.6700 \cdot 10^{6},\ \frac{\partial \tilde{h}}{\partial G_{i3}} = -0.8504 \cdot 10^{6}$$

$$\frac{\partial \tilde{h}}{\partial R_{01}} = 1.2039 \cdot 10^{-2},\ \frac{\partial \tilde{h}}{\partial R_{02}} = 0.5056 \cdot 10^{-2},\ \frac{\partial \tilde{h}}{\partial R_{03}} = 0.2634 \cdot 10^{-2}.$$

Altogether, these values provide the linear approximation $f_{\max} \approx 9429.9648$ for $G_{ik} = 10^{-6}$ S and $R_{0k} = 100$ Ω. This matches very well the actual value $f_{\max} = 9429.9679$ reported above. Note, however, that the computation of the individual sensitivities provides additional insight into the effect of the deviations of each parameter on the location of the peak frequency; specifically, both the input conductance and the output resistance of the summing stage are more relevant than the corresponding parameters of both integrators, as shown by the actual values obtained above for the different derivatives.

5 Concluding remarks

The use of a homogeneous formalism is essential in the analyses reported in this paper. This formalism makes it possible to provide closed form expressions for the transfer functions of two ports in a truly general manner, without the need to assume a specific description (admittance, impedance, etc.) in the circuit elements or to treat the different transfer functions separately. The key idea is to perform the analysis in terms of terminated two-ports, without restrictions on the form of the terminating devices: indeed, all independent sources, either ideal or nonideal, as well as short-circuit and open-circuit loads, can be handled in a uniform manner.

Classical and generalized cofactors formulae can be easily derived from our results. The attention has been restricted to the initial stages of the modeling process in order to provide analytical, matrix-theoretic formulae for the different transfer functions, but from the computational point of view the expressions obtained this way could be further improved by using symbolic circuit analysis techniques (see [7, 12, 17, 21, 25, 26, 27] and references therein). We have focused on the computation of transfer functions, but the same framework can be applied to the analysis of driving point immittances. Also, the results have been applied to the analysis of active filters but the approach seems to be well-suited for other applications.

Appendix

The integer constants $k_{\rm AB}$, $k_{\rm A}$ and $k_{\rm B}$ used in Section 3.1 (specifically, in Lemma 1) are presented and discussed in detail in [22], improving on previous results reported in [4]. We borrow from [22] the main properties of these constants, which capture some basic graph-theoretic properties of any reduced cutset (or incidence) matrix A and any reduced cycle matrix B of a given connected digraph.

Let us begin by recalling from digraph theory (cf. [2, 3, 4]) that the only maximal size, nonsingular (invertible) submatrices A_T of A are those defined by spanning trees; that is, the columns defined by the branches indexed by T yield a nonsingular submatrix A_T of order $n-1$ if and only if T specifies a spanning tree. Additionally, all such submatrices are known to have the same determinant in absolute value; that is, there is a positive integer k_A such that $\det A_T = \pm k_{\rm A}$ holds for all spanning trees. Essentially the same happens with any reduced cycle matrix B, once the spanning trees above are replaced by cotrees; that is, for maximal size submatrices B_C the relation $\det B_C \neq 0$ holds if and only if C specifies the branches of a cotree (the complementary set of a spanning tree); in this case, we have $\det B_C = \pm k_{\rm B}$ for a given positive constant $k_{\rm B}$.

Following the remarks above, the constants $k_{\rm A}$ and $k_{\rm B}$ can be formally defined as

$$k_{\rm A} = |\det A_T| \,, \quad k_{\rm B} = |\det B_C| \tag{49}$$

for any choice of a spanning tree T and a cotree C. In turn, a third, nonzero integer constant $k_{\rm AB}$ is defined in [22] as

$$k_{\rm AB} = (-1)^{\frac{n(n-1)}{2} + \sum_{j \in T} j} \det A_T \det B_{\overline{T}}, \tag{50}$$

for any spanning tree T and its cotree $\overline{T}$. This quantity is proved in [22] to be independent of the actual choice of T. Notice that $|k_{\rm AB}| = k_{\rm A} k_{\rm B}$, by construction (cf. (49)-(50)); hence $k_{\rm AB}$ equals either $+k_{\rm A}k_{\rm B}$ or $-k_{\rm A}k_{\rm B}$. We can also make use of this relation in the form $k_{\rm AB}^2 = k_{\rm A}^2 k_{\rm B}^2$.

By means of the Cauchy-Binet formula one can easily prove that

$$\det \left(A A^{\mathsf{T}} \right) = k_{\rm A}^2 \tau, \tag{51}$$

where τ is the total number of spanning trees in the digraph. In particular, one has $k_{\rm A} = 1$ if A is a reduced incidence matrix: in this case, (51) amounts to the well-known matrix-tree theorem (find background e.g. in [1]). Similarly, one has

$$\det \left(B B^{\mathsf{T}} \right) = k_{\rm B}^2 \tau. \tag{52}$$

Finally, the relation

$$\det \begin{pmatrix} A \\ B \end{pmatrix} = k_{\rm AB} \tau, \tag{53}$$

also holds (cf. (41) in [22]). This identity, which in essence results from a generalized Laplace expansion, explains why $k_{\rm AB}$ is chosen as indicated in (50). In this regard, note that (50) captures the (so to speak) exact sign relation between A and B; that is, it indicates what is the correct sign within the aforementioned relation $k_{\rm AB} = \pm k_{\rm A} k_{\rm B}$.

Acknowledgments

The author would like to thank Professor Álvaro de Guzmán Fernández, from ETSI Telecomunicación, Universidad Politécnica de Madrid, for several stimulating discussions on this topic.

Data

The text files Noninv-KHN-LowPass-Transfer-1.txt and Noninv-KHN-LowPass-Transfer-2.txt referred to in Section 4.3 are available from the author upon reasonable request.

References

[1] R. B. Bapat, *Graphs and Matrices*. New York: Springer-Verlag, 2010.

[2] B. Bollobás, *Modern Graph Theory*. New York: Springer-Verlag, 1998.

[3] J. A. Bondy and U. S. R. Murty, *Graph Theory*. New York: Springer-Verlag, 2008.

[4] W.-K. Chen, *Graph Theory and its Engineering Applications*. Singapore: World Scientific, 1997.

[5] W.-K. Chen, *Active Network Analysis*. Singapore: World Scientific, 2017.

[6] L. O. Chua, C. A. Desoer, and E. S. Kuh, *Linear and Nonlinear Circuits*. New York: McGraw-Hill, 1987.

[7] V. Filaretov and K. Gorshkov, "Efficient generation of compact symbolic network functions in a nested rational form", *Intl. J. Cir. Theory Appl.*, vol. 48, pp. 1032-1056, 2020.

[8] E. Fortuna, R. Frigerio and R. Pardini, *Projective Geometry*. Cham, Switzerland: Springer, 2016.

[9] S. Franco, *Design with Operational Amplifiers and Analog Integrated Circuits*. New York: McGraw-Hill, 2015.

[10] J. Gallier, *Geometric Methods and Applications*. New York: Springer, 2011.

[11] P. R. Gray, P. J. Hurst, S. H. Lewis and R. G. Meyer, *Analysis and Design of Analog Integrated Circuits*. Hoboken, New Jersey: Wiley, 2009.

[12] O. Guerra, E. Roca, F. V. Fernández and A. Rodríguez-Vázquez, "Approximate symbolic analysis of hierarchically decomposed analog circuits", *Analog Integr. Circuits Signal Process.*, vol. 31, pp. 131-145, 2002.

[13] R. A. Horn and Ch. R. Johnson, *Matrix Analysis*. Cambridge: Cambridge University Press, 2013.

[14] P. Horowitz and W. Hill, *The Art of Electronics*. New York: Cambridge University Press, 2015.

[15] R. C. Jaeger and T. N. Blalock, *Microelectronic Circuit Design.* New York: McGraw-Hill, 2016.

[16] G. R. Kirchhoff, "Ueber die Auflösung der Gleichungen, auf welche man bei der Untersuchung der linearen Vertheilung galvanischer Ströme geführt wird", *Annalen der Physik und Chemie*, vol. 72, pp. 497-508, 1847 . English translation: "On the solution of the equations obtained from the investigation of the linear distribution of galvanic currents", *IRE Tr. Circuit Theory*, vol. 5, pp. 4-7, 1958.

[17] S. Lasota, "Symbolic analysis of electric networks with higher order summative cofactors and parameter decision diagrams", *Int. J. Cir. Theory Appl.*, vol. 46, pp. 1796-1826, 2018.

[18] Z. S. Madonsela and V. M. Srivastava, "Design and modelling of analysis of Kerwin, Huelsman, and Newcomb (KHN) biquad filter using double-gate MOSFET for low energy devices", *Intl. J. Eng. Trends Techn.*, vol. 71, pp. 181-195, 2023.

[19] J. C. Maxwell, *A Treatise on Electricity and Magnetism.* Oxford: Clarendon Press, 1873.

[20] S. A. Pactitis, *Active Filters. Theory and Design.* Boca Raton: CRC Press, 2007.

[21] Z. Qin, S. X. D. Tan and C.-K. Cheng, *Symbolic Analysis and Reduction of VLSl Circuits.* New York: Springer, 2005.

[22] R. Riaza, "Circuit theory in projective space and homogeneous circuit models", *IEEE Trans. Circuits Syst. I*, vol. 66, pp. 463-476, 2019.

[23] R. Riaza, "An abstract modeling framework for one- and two-ports", *Intl. J. Cir. Theory Appl.*, vol. 53, pp. 4842-4861, 2025.

[24] I. R. Shafarevich and A. O. Remizov, *Linear Algebra and Geometry.* Berlin: Springer-Verlag, 2013.

[25] G. Shi, "A survey on binary decision diagram approaches to symbolic analysis of analog integrated circuits", *Analog Integr. Circuits Signal Process.*, vol. 74, pp. 331-343, 2013.

[26] G. Shi, "Two-graph analysis of pathological equivalent networks", *Intl. J. Cir. Theory Appl.*, vol. 43, pp. 1127-1146, 2015.

[27] G. Shi, S. X.-D. Tan and E. Tlelo Cuautle, *Advanced Symbolic Analysis for VLSI Systems.* New York: Springer, 2014.

[28] G. C. Temes and J. W. LaPatra, *Introduction to Circuit Synthesis and Design.* New York: McGraw-Hill, 1977.